

# NONLINEAR OPTIMIZATION OF CLIC DRS NEW DESIGN WITH VARIABLE BENDS AND HIGH FIELD WIGGLERS

H. Ghasem<sup>\*§</sup>, F. Antoniou, J. Alabau-Gonzalvo, S. Papadopoulou, Y. Papaphilippou,  
CERN, Geneva, Switzerland

<sup>§</sup> School of Particles and Accelerator, IPM, Tehran, Iran

## Abstract

The new design of CLIC damping rings is based on longitudinal variable bends and high field superconducting wiggler magnets. It provides an ultra-low horizontal normalised emittance of 412 nm-rad at 2.86 GeV. In this paper, nonlinear beam dynamics of the new design of the damping ring (DR) with trapezium field profile bending magnets have been investigated in detail. Effects of the misalignment errors have been studied in the closed orbit and dynamic aperture.

## INTRODUCTION

The CLIC damping rings aim to reduce the horizontal and vertical natural emittance of the incoming electron and positron beams to less than 100 and 1 pm, respectively, at 2.86 GeV while keeping the ring as compact as possible. They are an essential part of the linear collider, for producing and delivering the ultra-high beam brightness necessary for the luminosity performance of the collider.

The DRs' layout has a racetrack shape and consists of two arcs and two long straight sections (LSS). The arcs are composed of theoretical minimum emittance (TME) cell with longitudinally variable bends and the straight sections are based on FODO cell filled with high field superconducting damping wigglers. The required space is also reserved for the RF cavities, injection and extraction components and vacuum equipment. Each arc section includes of 42 TME cells and there are totally 96 dipoles in the whole DR. In addition to the horizontal defocusing strength in dipoles, two families of quadrupole (one focusing and one defocusing) are employed to perform beam focusing in the TME cell. There are 10 FODO cells per straight section and each FODO cell is filled with two optimized Nb3Sn high field superconducting damping wigglers. The wiggler with total length of 2 m, period length of 49 mm, provides a high magnetic field of 3.5 T. The optical functions between the arcs and the straight sections are well matched using dispersion suppressors (DSs) and beta matching sections.

## LONGITUDINAL VARIABLE DIPOLES

The longitudinally variable dipole can provide lower horizontal emittances than a uniform dipole of the same bending angle [1-5]. For this propose, the maximum magnetic field of a variable bend should be applied at its center and decrease towards the two exit edges of the dipole. In this case, the bending radius of a variable bend

will have an evolution similar to the one of the uniform dipole's dispersion invariant  $H(s)$  [4-8].

Several longitudinal field profiles of dipoles and corresponding designed DR parameters have been studied [4,9]. In this paper a field profile with trapezoidal evolution of the bending radius is used. The schematic evolution of dipole magnetic field ( $B$ ) and bending radius ( $\rho$ ) for the trapezium field profile dipole are shown in Fig. 1. As displayed, the trapezium field profile dipole is characterized using two lengths of  $L_1$  and  $L_2$  with corresponding different bending radii of  $\rho_1$  and  $\rho_2$ .

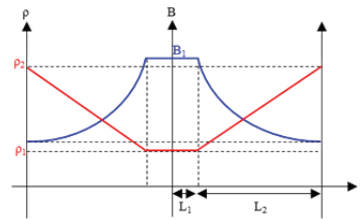


Figure 1. The schematic evolution of the magnetic field and bending radius in the trapezium profile dipole. The sum of  $L_1$  and  $L_2$  is equal to the half dipole length.

Many compromises between the several parameters of the DR such as emittance, phase advance and chromaticity had to be taken into account for the good optimization of each dipole section of the trapezium field profile bend [5,8]. We ended up with an optimized trapezium field profile dipole with total length of 58 cm and bending angle of 4 degrees.

## DAMPING RING

The main parameters of the designed damping ring are given in Table 1. The optical functions in the TME/FODO cell are shown in Fig. 2.

Table 1. Main Parameters of CLIC DR

Parameters	Value
Energy (GeV)	2.860
Circumference (m)	359.440
Tune (-/-)	45.291/8.317
Natural emittance (pm.rad)	73.752
Natural chromaticity	-128.789/-61.832
1 <sup>st</sup> order mom. com. factor	1.248E-4
Energy spread	1.275E-3
Energy loss per turn (MeV)	5.721
Damping time (ms/ms/ms)	1.179/1.199/0.604

The optics of the TME and FODO cells are well matched with use of the dispersion suppressors grouped within two

\* hossein.ghasem@cern.ch

types. The first type (type-I) matches the optics at the end of arc section to the optics at the beginning of the straight section and the second type (type-II) is just a mirror symmetric cell, see Fig. 2.

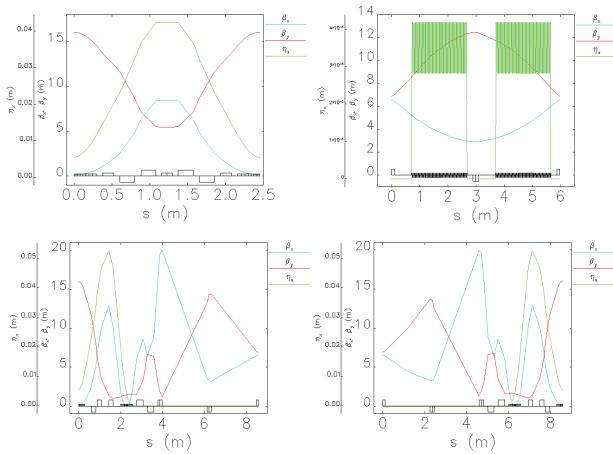


Figure 2. The optical functions in the (left-top) TME cell and (right-top) FODO cell (left-bottom) DS type-I and (right-bottom) Ds type-II.

### NONLINEAR BEAM DYNAMICS

Two families of sextupole magnets both with the same length of 15 cm in the TME cell are considered to correct the natural chromaticity of ring to +1. The particle tracking has been performed over 2000 turns through the damping ring. The dynamic aperture (DA) of the both electron and positrons damping rings are computed with the ELEGANT code [10] and the 4D tracking results for the on/off energy particles are given in Fig. 3. The normalized horizontal and vertical sizes of the incoming beams at the point of calculation have been mentioned in the plots. Regarding the fact that the magnets fringe fields are taken into account while the magnet error effects are neglected, the resulted DA seems to be comfortable enough for both rings. Figure 4 shows the initial positions of the on energy electron/positron particles that get lost during tracking. Tune point variation with energy deviation has been studied and the results are given in Fig. 5. It represents a very small variation of the tune point up to  $\pm 0.3\%$  energy deviation and reveals that the present sextupole arrangement was a good starting point to perform nonlinear beam dynamics of the new design of damping ring based on trapezium field profile dipole.

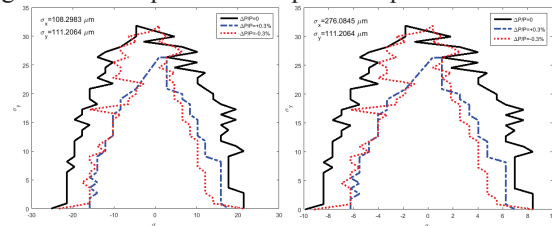


Figure 3. The dynamic aperture for the (left) electron and (right) positron damping rings.

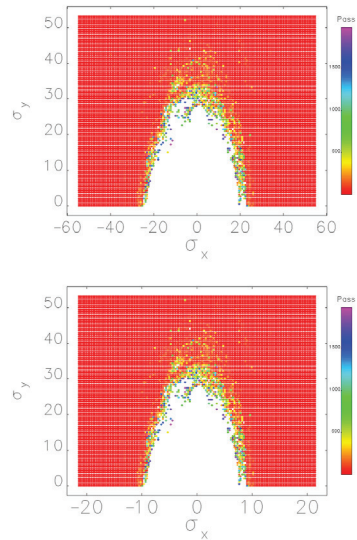


Figure 4. The on energy (top) electron and (bottom) positron particles which get lost during tracking, color coded with the turn number.

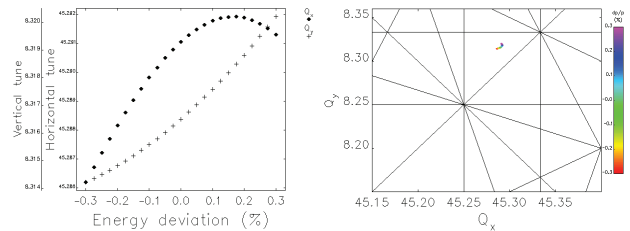


Figure 5. (left) Tune shift with energy deviation and (right) corresponding tune diagram.

The diffusion map and corresponding frequency map analysis are depicted in Fig. 6 which indicate that the tune shift for about  $\pm 2.5$  mm physical space is close to 0.25. In order to reduce the tune spread with amplitude, it is proposed to increase the families of sextupole from 2 to 4 or use of the octupole magnets which both issues are under further study.

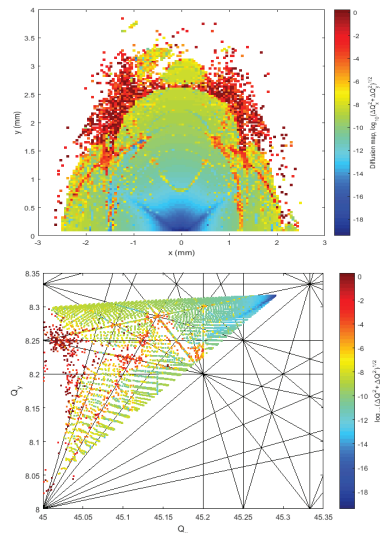


Figure 6. (top) The dynamic aperture with respect to tune diffusion and (bottom) corresponding tune diagram.

### EFFECTS OF ERRORS

Several seeds of alignment and magnet strength errors have been imposed randomly into the DR lattice to study their effects on the closed orbit and the dynamic aperture. The errors are listed in the Table 2.

Table 2. The errors imposed in the DR lattice. The errors have been cut off at one sigma.

Errors	value
Hor./Ver. misalignment of dipole, sextupole, wiggler, BPM	$\pm 50 \mu\text{m} / \pm 50 \mu\text{m}$
Hor./Ver. misalignment of quad.	$\pm 8 \mu\text{m} / \pm 8 \mu\text{m}$
Roll of magnets	$\pm 0.1 \text{ mrad}$
Fraction of quadrupole strength	5E-4
Fraction of sextupole strength	1E-4

In order to correct the orbit, 262 horizontal correctors (HCOR) and 242 vertical correctors (VCOR) are used. In addition, 262 BPMS are employed in the lattice and they are placed in the proper phase advances. The location of the HV correctors and BPMS in the TME cell, FODO cell and both types of dispersion suppressors are plotted in Fig. 7. The corrected orbit along the ring is shown in Fig. 8. It is found that the corrected orbit is sensitive to the misalignment of quadrupole and its displacement of above  $\pm 8 \mu\text{m}$  cannot be tolerated. The maximum strength of correctors used for orbit correction is 0.45 mrad.

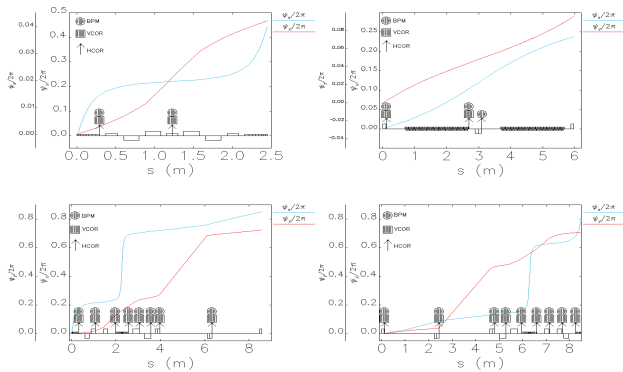


Figure 7. Location of HV correctors and BPMS in (top-left) FODO cell, (top-right) TME cell, (bottom-left) type-I DS and (bottom-right) type-II DS.

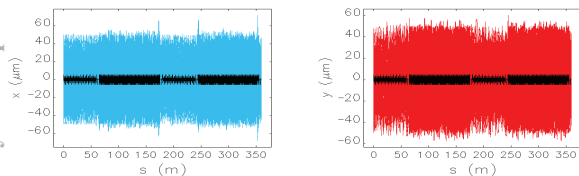


Figure 8. The (left) horizontal and (right) vertical corrected closed orbit along the ring for 100 seeds of errors.

The dynamic aperture in the presence of errors mentioned in Table 2 have been evaluated for 50 seeds and then the particles have been tracked 500 turns in the ring for this calculation. The results shown in Fig. 9 indicate that there are still enough physical stable space up to around  $\pm 7.4\sigma_x / \pm 7.2\sigma_y$  and  $\pm 2.9\sigma_x / \pm 7.2\sigma_y$  for the electron and

positron damping rings respectively. The DA for the positron DRs in the horizontal plane is quite small and need further optimisation.

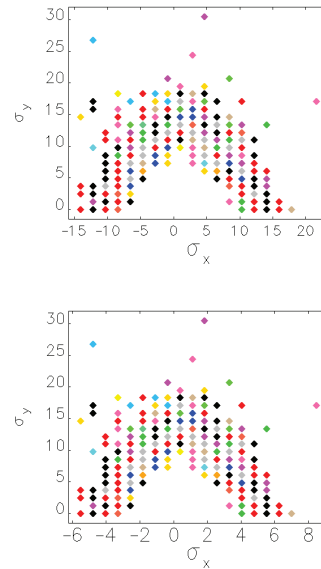


Figure 9. Dynamic aperture in the presence of the errors mentioned in Table 2, (top) for the electron and (bottom) for the positron damping rings.

### CONCLUSION

The nonlinear beam dynamics have been studied for the new design of the CLIC DR with trapezium field profile dipole. Two families of sextupoles are employed to correct the natural chromaticity. Particle tracking with and without errors have been performed and the results show that the present sextupole arrangement was a good starting point for nonlinear optimization. However, in order to make the dynamic aperture larger with less tune dependence, use of four families of sextupole or using octupole magnet is under further study.

### ACKNOWLEDGMENT

The research leading to these results has received funding from European Commission under the FP7 Research Infrastructures project EuCARD-2.

### REFERENCES

- [1] J. Guo and T. Raubenheimer, *Low Emittance e-/e+ Storage Ring using Bending Magnets with Longitudinal Gradient*, proc. of EPAC 2002, Paris, France (2002) p. 1136-1138.
- [2] R. Nagaoka, A.F. Wrulich, *Emittance minimisation with longitudinal dipole field variation*, Nucl. Instrum. Methods Phys. Res., Sect. A 575 (2007) p. 292-304.
- [3] A. Streun, *The anti-bend cell for ultralow emittance storage ring lattices*, Nucl. Instrum. Methods Phys. Res., Sect. A, 737 (2014) p. 148-154.
- [4] Y. Papaphilippou, P. Elleaume, *Analytical Considerations for Reducing the Effective Emittance with Variable Dipole Field Strengths*, proc. of PAC 2005, Tennessee, USA (2005) p. 2086-2088.

- [5] S. Papadopoulou, F. Antoniou, Y. Papaphilippou, *Alternative optics design of the CLIC damping rings with variable dipole bends and high-field wigglers*, proc. of IPAC 2015, Virginia, USA (2015) p.2046-2049.
- [6] C.-x Wang, Y. Wang, Y. Peng, *Optimal dipole-field profiles for emittance reduction in storage rings*, PRST-AB 14, 034001(2011).
- [7] C.-x Wang, *Minimum emittance in storage rings with uniform or nonuniform dipoles*, PRST-AB 12, 061001 (2009).
- [8] S. Papadopoulou, F. Antoniou and Y. Papaphilippou, *Emittance reduction with variable bending magnet strengths: Analytical optics considerations*, preprint (2016).
- [9] A. Streun, A. Wrulich, *Compact low emittance light sources based on longitudinal gradient bending magnets*, Nucl. Instrum. Methods Phys. Res., Sect. A, 770 (2015) p. 98-112.
- [10] M. Borland, *Elegant: a flexible sdds-compliant code for accelerator simulation*, Advanced Photon Source, Argonne National Laboratory, USA, Report No. LS-287, 2000.